

Supplemental Information

Using Chimeric Mice with Humanized Livers to Predict Human Drug Metabolism and a Drug-Drug Interaction

Toshiko Nishimura^{1*}, Yajing Hu^{1*}, Manhong Wu¹, Edward Pham², Hiroshi Suemizu³, Menashe Elazar², Michael Liu², Ramazan Idilman⁵, Cihan Yurdaydin⁵, Peter Angus⁶, Catherine Stedman⁷, Brian Murphy⁸, Jeffrey Glenn², Masato Nakamura³, Tatsuji Nomura³, Yuan Chen⁴, Ming Zheng¹, William L. Fitch¹, and Gary Peltz^{1#}

***In vitro* characterization of clemizole metabolism.** To characterize the metabolic pathways and the basis for the inter-species differences, a detailed *in vitro* analysis of clemizole metabolism was performed. First, the metabolites formed after clemizole was incubated with mouse rat and human microsomes were determined as described in the supplemental information. Clemizole exhibited much greater stability in human microsomes, where it is largely metabolized on the pyrrolidine ring to form one major metabolite, the lactam, **M1**. Clemizole is more rapidly metabolized by rodent microsomes to multiple different metabolites (**M8, M9**), but very little **M1** was formed (**Figure S2, Tables S1, S2**). Since intact liver cells can generate more complex metabolites, the profile of clemizole metabolites formed after incubation with human and rat hepatocytes was next characterized (**Table S2**). M1 was the major metabolite formed after incubation with human hepatocytes; and smaller amounts of M14 (the glucuronide of M4) and M6, which is a ring-opened pyrrolidine oxidation product, were also formed. However, rat hepatocytes produced a very different pattern of clemizole metabolites; M15 (the glucuronide of M9) was the major metabolite and lesser amounts of other Phase 2 metabolites (M16-M19) were also formed. It is noteworthy that none of the rodent *in vitro* systems identified the major clemizole metabolites (M12, M14) that were produced by mice *in vivo*. Then, CYP450 reaction phenotyping indicated that clemizole could be metabolized by a variety of human CYP450 enzymes (described in the supplement and **Figure S3**). Taken together, the recombinant CYP450 enzyme and microsome data indicate that in human liver

clemizole is primarily converted to intermediate 'A' (Figure 2). Then, several CYP450 enzymes (CYP3A4, CYP2C19 or CYP2D6) could further oxidize this intermediate to M1; while CYP2C9 or CYP1A2 can produce M2, but they cannot produce M1; and CYP2C9 appears to be the only source for M4. After considering the relative CYP450 abundance and other factors (Proctor et al., 2004), the extrapolated data indicate that CYP3A4 and CYP2C9 account for 53% and 30%, respectively, of the human Phase 1 metabolism of clemizole; while CYP2D6 and CYP2C19 each contribute to ~5-10% of clemizole metabolism. The ability of ritonavir, which is an inhibitor of CYP3A4 activity, to inhibit clemizole metabolism *in vitro* is consistent with these results, and indicates that CYP3A4 plays a major role in clemizole metabolism (**Figure S4**). M1 is the predominant human drug metabolite because CYP3A4 is the most abundantly expressed (60% of total) hepatic CYP450 enzyme (Danielson, 2002). Although rodent CYP450 phenotyping was not performed, clemizole metabolism in rodents must be dominated by a CYP2C-type of aromatic oxidation reaction that produces the rodent predominant metabolites (M12, M14 and M15) shown in Figure 2.

Analysis of the structure of clemizole metabolites. Clemizole has three sites that are susceptible to Cytochrome P450 oxidation: the pyrrolidine, the benzimidazole and the linker between them. The chlorobenzyl group is stable to metabolism. The metabolites were identified based on their collision-induced dissociation (CID) behavior in tandem mass spectrometry, accurate mass and retention time. Table S1 lists the structures and relevant LC/MS/MS information. Figure 2 shows the structures of clemizole and its metabolites, and its metabolic pathways. All metabolites had an observed accurate mass within 2.8 ppm of the predicted accurate mass. Clemizole fragments upon CID to yield a predominate ion at m/z 255, due to loss of pyrrolidine. This ion is moved to m/z 271 in the aromatic ring oxidized metabolites. Clemizole also has a major CID fragment at m/z 125 that represents the chlorobenzyl cation and is unchanged in all metabolites. The predominant metabolite produced by human

microsomes M1 had a molecular ion 14 Da greater than clemizole, and the m/z 125 fragment ion with CID, which indicated the oxidation had occurred on the pyrrolidine; As M1 had a longer retention time than clemizole in reverse phase LC, this metabolite, is identified as the lactam. M2 has a molecular weight 2 Da less than clemizole so it is drawn as the dehydro metabolite. The aminol metabolite A initially formed via alpha-oxidation in the pyrrolidine was not observed here; it may be unstable during LC/MS to produce M2; or it may be further oxidized to form M1, M3 or M6 *in vitro* and *in vivo*. M3 is the primary amine formed via further oxidation of A or M6 possibly through unstable intermediate B. In CID M3 loses ammonia predominately to give m/z 255. M4 and M10 are mono-hydroxylation metabolites. M4, with its indicative CID fragment moved to m/z 271 and a short retention time, is drawn with oxidation on the benzimidazole although the exact regiochemistry is not certain. M10 is drawn as the N-oxide as it's retention time is similar to clemizole and it's CID main indicative fragment is at m/z 256/257 (N-oxides typically lead to altered CID patterns including radical species (Fitch et al., 2007).) M5 with an even-to-odd mass shift (due to nitrogen loss) is drawn as the primary alcohol that could be formed by reduction of an aldehyde, which would initially form if bridgehead oxidation and loss of pyrrolidine occurred. M6 is an amino acid likely formed via further oxidation of the unstable metabolite A. M6 is of higher abundance in hepatocyte incubations and *in vivo*. M7 and M9 are isomeric doubly oxidized metabolites with a net increase of +30 Da. M7 has dual oxidations on the pyrrolidine ring with its indicative fragment at m/z 255 along with a dominant water loss fragment. M9 combines the features of M1 and M4 with its indicative fragment at m/z 271. M8 combines the features of M4 and M5 with the characteristic m/z 271 ion due to water loss. M11 combines the features of M3 and M4 with the indicative fragment at m/z 271. M12 is a metabolite mainly observed *in vivo*; it has a molecular formula consistent with a complete loss of the pyrrolidinylmethyl side chain possibly via further oxidation of M3 or M5.

The identification of metabolites produced in hepatocyte incubations was conducted with an LTQ Orbitrap so MS³ data is listed for these metabolites. MS³ is very useful for identifying Phase 2 metabolites because in the first stage of CID the glucuronide (or sulfate) is removed so the MS³ spectrum of a Phase 2 metabolite is identical to the MS/MS spectrum of the corresponding Phase 1 metabolite. M13 is a glucuronide of the parent drug, which was only observed after incubation with human hepatocytes. It is likely a quaternary N-glucuronide of the pyrrolidine, a pathway that is often lacking in rodents (Chiu and Huskey, 1998). M14 has the [M+H]⁺ consistent with a mono-oxidation and a glucuronidation. In MS/MS M14 gave rise to fragment ions at m/z 342 and 271 consistent with it being the glucuronide of M4. M15 has the [M+H]⁺ consistent with a double-oxidation and a glucuronidation. In MS/MS M15 gave rise to fragment ions at m/z 356 and 271 consistent with it being the glucuronide of M9. M16 is a glucuronide of M7 with the characteristic m/z 255 fragment ion. M17 is an acyl glucuronide of M6. M18 is a minor rat-specific glucuronide of a triply oxidized phase 1 metabolite (not observed unconjugated). M19 is a rat-specific glutathione conjugate with a mass consistent with glutathione trapping from an arene oxide reactive intermediate on the pathway to M9.

Recombinant Cyp450 reaction data. The data shown in Figure S3 indicates that multiple CYP450 are involved in the clemizole metabolism. Clemizole was rapidly metabolized after incubation with CYP2C9, CYP2C19, CYP2D6, or CYP3A4; and with CYP1A2 to a lesser extent. After other factors such as CYP450 abundance and differences in intrinsic activity between the recombinant system and human liver microsomes are incorporated (Proctor et al., 2004), the extrapolated data indicates that CYP3A4 and CYP2C9, are the major CYP450 isoforms that could account for 53% and 30%, respectively, of the Phase 1 metabolism of clemizole; while CYP2D6 and CYP2C19 are each responsible for ~5-10% of clemizole metabolism. A more detailed structural (QTRAP MRM-EPI) analysis of metabolites produced after incubation with 10 uM clemizole confirms that multiple metabolites were formed after clemizole was incubated with

each of the different CYP isoforms (**Table S3**). CYP3A4 is primarily responsible for production of metabolites M1 and M2; CYP2C9 for M2 and M4; CYP2D6 for M1 and M2; CYP2C19 for M2; and CYP1A2 for M2 and M4. Taken together, this data indicates that in human liver clemizole is converted to intermediate A (Figure 2) *in vitro*. CYP3A4, CYP2C19 and CYP2D6 can further oxidize this intermediate to M1; while in the presence of CYP2C9 or CYP1A2, M2 is generated, but they cannot produce M1. Cyp2C9 appears to be the only source of M4.

Supplemental Materials and Methods

Chemicals and reagents. For *in vitro* and animal experiments, clemizole hydrochloride and omeprazole were purchased from Sigma (St. Louis, MO); ritonavir was purchased from Santa Cruz Biotechnology (Santa Cruz, CA). Pooled Human liver microsomes, male rat and mouse liver microsomes were purchased from BD Gentest (Woburn, MA). Cryopreserved human hepatocytes and recombinant CYP450 enzymes were purchased from BD Biosciences (San Jose, CA, USA). Rat hepatocytes were freshly isolated according to standard procedures. All other chemicals were purchased from commercial sources and were of the highest purity available.

Mouse pharmacokinetic studies. All animal experiments were performed using protocols approved by the Stanford Institutional Animal Care and Use Committee. Male C57BL6/J mice (8 weeks of age) were obtained from Jackson Labs and housed for 2 weeks prior to experimentation. NOG mice were obtained from In Vivo Sciences International (Sunnyvale, CA). Chimeric TK-NOG mice with humanized livers were prepared exactly as described (Hasegawa et al., 2011), except the Gancyclovir dose was increased to 25 mg/kg, which was administered 7 and 5 days prior to human liver cell transplantation. For transplantation, freshly isolated or cryopreserved human hepatocytes were obtained from Celsis In Vitro Inc. (Baltimore, MD) and

Life Technologies (Grand Island, NY). The characteristics of the human hepatocyte donors are described in **Table S4**. The pharmacokinetic studies using these mice were performed 8-12 weeks after transplantation of the human liver cells. Control NOG mice and humanized TK-NOG mice were administered 25 mg/kg clemizole PO, and blood samples were collected 30 minutes after dosing. The C57BL/6J mice (3 per time point) were dosed with 25 mg/kg PO Clemizole, and blood samples were collected at 15, 30 min and 1, 2, 4 and 6 hrs after dosing for analysis. For the drug-drug interaction studies, eight humanized TK-NOG mice were dosed with Clemizole (25 mg/kg P.O.) with or without ritonavir (20 mg/kg P.O), and blood samples were collected 30 minutes after dosing. Six of these mice were also treated with debrisoquine (10 mg/kg PO), in the presence or absence of ritonavir (20 mg/kg PO), and plasma obtained 2 hrs later for analysis.

Statistical analysis of mouse pharmacokinetic data. To assess the statistical significance of the difference in the relative amount of each metabolite (clemizole, M1, M2, M6, M12, M14 and M15) in plasma obtained from control and humanized TK-NOG mice, a two-sample two-sided t test was used. Of note, the amount of M1 was < 7 in all 8 of the control mice, while it was > 7 in all but one of the humanized TK-NOG mice. The two-sample two-sided t test result indicated that this difference in M1 abundance was highly significant (p value = 0.0004). In the DDI studies, a paired-sample t test was used to compare the amount of each of the metabolites (Figure 2) and for the clemizole AUC (0-12hr) (Figure 3) measured in the presence and absence of ritonavir co-administration. The paired-sample t test was also used to compare the relative amounts of 4-OH debrisoquine in the 6 humanized TK-NOG mice measured in the presence or absence of ritonavir co-administration.

Quantitative analysis of clemizole and metabolites in plasma. Mouse plasma (50 μ L) was treated with acetonitrile with 0.1% formic acid (200 μ L), vortexed and incubated at -20°C for one

hour, centrifuged at 10,000 rpm for 10 min. The supernatants were collected, dried and resuspended in 50uL 5% acetonitrile with 0.1% formic acid for the analysis by LC/MS. HPLC was performed using an Agilent 1200 column compartment, capillary pump, and an autosampler on a Zorbax C18 column, 0.5x150 mm. The flow rate was 20 mL/min with a gradient from 5% solvent B (acetonitrile with 0.1% formic acid; solvent A is 0.1% formic acid in water) to 95% B in 30 min and held at 95% B for 5 min. Mass spectrometric analysis were carried out on an Agilent Model 6520 qTOF mass spectrometer equipped with an ESI source. The heated capillary temperature in the source was held at 325°C. Full scan (m/z 110–1000) spectra or data dependent MS/MS spectra were collected. The metabolites were identified based on their collision-induced dissociation behavior in tandem mass spectrometry, accurate mass and retention time. Quantitative analysis of clemizole was performed using a calibration curve at 9-1257 ng/ml clemizole spiked into blank mouse plasma and extracted as above. An internal standard 1-(p-bromobenzyl)-2-(1-pyrrolidinylmethyl)- Benzimidazole was also spiked in at 1000ng/ml. Relative amounts of clemizole and metabolites in each sample were calculated using the assumption that all compounds had the same MS response factor.

Human pharmacokinetic and metabolite studies. Phase 1b studies (to be reported elsewhere) were conducted in genotypes 1 and 2 HCV patients under IRB-approved protocols to investigate the safety and tolerability, pharmacokinetics, and pharmacodynamics of clemizole HCl (see www.Clinicaltrials.gov and approval by the University of Ankara Medical School Ethics Committee; study sponsor Eiger BioPharmaceuticals, Inc.). De-identified aliquots of excess material, which were not needed for clinical monitoring, were kindly provided by Wenjin Yang (Eiger BioPharmaceuticals, Inc.) to us for PK and metabolite analysis. The samples obtained were from human subjects that were administered 100 mg Clemizole P.O., with or without 100 mg ritonavir P.O. administered one hour before the clemizole, and blood samples were obtained 0 to 12 hrs after dosing. The relative abundance of clemizole and its metabolites in plasma

were measured in samples obtained from 10 patients treated with clemizole alone, and from 3 patients who participated in the subcomponent evaluating the effect of ritonavir co-administration, by LC/MS analysis as described below.

Microsome incubations and analysis. Clemizole (20 μ M, diluted from 10 mM stock in DMSO) was mixed with human, rat or mouse liver microsomal proteins (1 mg/ml) in 100 mM potassium phosphate buffer (pH 7.4) supplemented with 1 mM glutathione and 5 mM $MgCl_2$ in a total volume of 1 ml. After 5 min pre-incubation at 37°C, the reactions were initiated by addition of 2 mM NADPH, and then quenched by addition of 1 mL ice cold acetonitrile after 60 min. Negative control samples contained NADPH with test compound added with the acetonitrile quench. HPLC was performed using an Agilent 1200 column compartment, capillary pump, and autosampler on a Zorbax C18 column, 0.5x150 mm. The flow rate was 20 μ L/min with a gradient from 5% solvent B (acetonitrile with 0.1% formic acid; solvent A is 0.1% formic acid in water) to 95% B in 30 min and held at 95% B for 5 min. Mass spectrometric analysis were carried out on an Agilent Model 6520 quantitative Time Of Flight mass spectrometer equipped with an ESI source. The heated capillary temperature in the source was held at 325°C. Full scan (m/z 110–1000) spectra or data dependent MS/MS spectra were collected. The metabolites were identified based on their collision-induced dissociation behavior in tandem mass spectrometry, accurate mass and retention time. Relative amounts of clemizole and metabolites in each sample were calculated using the assumption that all compounds had the same MS response factor.

Hepatocyte incubations. Using wide-bore pipette tips, aliquot 0.1 mL cell suspension into a 24 well plate, and the plates were incubated for at least 0.5 hr in a 37 °C incubator on shaker (500 rpm). Two wells of volume 0.5 mL were run for each test compound. Incubation mixtures (0.5 mL) contained test compound (20 μ M with a maximum of 1% dimethyl sulfoxide used as

cosolvent) in Gibco HepatoZYME (Invitrogen, Carlsbad, CA, USA) media supplemented with 5% fetal bovine serum and 2mM L-glutamine and were allowed to react for 4 h. All incubations were quenched with an equal volume of acetonitrile, the duplicate wells combined, followed by centrifugation, evaporation to dryness and reconstitution in 10% acetonitrile in water. Negative control samples contained test compound only added with the acetonitrile quench. HPLC was performed using an Agilent (Santa Clara, CA, USA) 1100 column compartment, binary pump, autosampler and diode-array detector on a Varian (Palo Alto, CA, USA) Polaris 5 micron, C18-A column, 2.1x250 mm, in a column heater at 55°C. The flow rate was 0.3 mL/min with a gradient from 0%(after a 5 min hold) solvent B (acetonitrile with 0.1% formic acid; solvent A is 0.1% formic acid in water) to 30% B in 25 min and held at 95% B for 5 min. Mass spectrometric analysis were carried out on a Thermo-Fisher (San Jose, CA, USA) LTQ Orbitrap mass spectrometer equipped with an ESI source. The heated capillary temperature in the source was held at 250°C. Full scan positive spectra were collected along with MS/MS spectra for the major two peaks with the Orbitrap. Corresponding positive ion MS³ spectra were collected with the LTQ low resolution detector. Negative full scan (m/z 180–900), MS/MS and MS³ spectra were collected with the LTQ low resolution detector. Relative quantitative analyses were based on UV integration (276 nm) of identified peaks.

CYP reaction phenotyping. The reaction phenotyping was conducted using cDNAs expressing recombinant hCYP450 enzymes. (rhCYP 1A2, 2C8, 2C9, 2C19, 2D6, 3A4) and control preparations from baculovirus-infected Sf9 insect cells (supersomes) that were purchased from BD Gentest (Woburn, MA). Cytochrome c reductase was co-expressed in all preparations, and cytochrome b5 was expressed in cDNA-expressed CYP2C8, 2C9, 2C19, and 3A4. Incubation mixtures were prepared containing potassium phosphate buffer (50 mM, pH 7.4), magnesium chloride (5 mM), rhCYP450 enzymes (varied CYP concentration at pmole/ml with total 0.5 mg protein/ml), and clemizole (1 μM). The reaction mixtures were pre-incubated at 37°C for five

minutes prior to initiation of reactions with NADPH (2 mM final concentration) and stopped by addition of acetonitrile (1:1 by volume) at pre-determined time points (0, 5, 10, 20 min). Following quenching, one volume of sample was transferred to an injection plate containing one volume acetonitrile/water with internal standard. Samples were centrifuged at 3000 rpm for 10 min and the supernatants were collected for the analysis by LC/MS. Quantitative analysis of clemizole depletion was conducted using LC/MS/MS on an ABI 4000 mass spectrometer using MRM (m/z 326 to m/z 255) with sample introduction on LC system containing a Shimadzu 20ADP binary pumps (Columbia, MD) and HTC PAL autosampler (Leap Technologies, Cary, NC), and a Hypersil C18 column (2.1x50 mm). The flow rate was 0.4 mL/min with a gradient from 5% (after a 1 min hold) solvent B (Acetonitrile: Methanol (50:50) with 0.1% Formic Acid) and 95% solvent A (5 mM Ammonium Acetate with 0.1% Formic Acid) to 90% B in 3 min and held at 90% B for 1 min. Formation of predicted metabolites (m/z 326 to m/z 255 for parent; 340 to 255 for M1; 342 to 271 for M4; 324 to 255 for M2) were monitored on ABI 4000 QTrap mass spectrometer using the using multiple reaction monitoring triggered enhanced product ion scanning to obtain representative MS/MS spectra for the major metabolites (MRM-EPI). The LC method is similar as previously described, except for the column and run time. A Hypersil C18 column, 2.1x100mm, was used and total run time is 25 min.

Supplemental References

- Chiu SH, Huskey SW (1998) Species differences in N-glucuronidation. *Drug Metab Dispos* 26:838-847.
- Danielson PB (2002) The cytochrome P450 superfamily: biochemistry, evolution and drug metabolism in humans. *Curr Drug Metab* 3:561-597.
- Fitch WL, He L, Tu YP, Alexandrova L (2007) Application of polarity switching in the identification of the metabolites of RO9237. *Rapid Commun Mass Spectrom* 21:1661-1668.
- Hasegawa M, Kawai K, Mitsui T, Taniguchi K, Monnai M, Wakui M, Ito M, Suematsu M, Peltz G, Nakamura M, Suemizu H (2011) The reconstituted 'humanized Liver' in TK-NOG mice is mature and functional. *Biochem Biophys Res Commun* 405:405-410.
- Proctor NJ, Tucker GT, Rostami-Hodjegan A (2004) Predicting drug clearance from recombinantly expressed CYPs: intersystem extrapolation factors. *Xenobiotica* 34:151-178.

Supplemental Table 1. LC/MS Characterization of clemizole and its metabolites. The retention times were measured using the hepatocyte LC method, and were adjusted for those few metabolites that were only detected *in vivo* or after incubation with microsomes.

Metabolite	Retention time	Nominal [M+H] ⁺	PPM error	Indicative MS/MS fragments	Indicative MS ³ fragments
Clemizole	14.0	326	2.8	255,125	220
M1	15.2	340	1.8	255,125	
M2	13.2	324	2.8	255,125	
M3	12.8	272	0.7	255,125	
M4	12.2	342	0.3	271,255	
M5	12.7	273	1.1	255,125	
M6	13.3	358	1.1	340,125	255
M7	14.0	356	2.2	338,255,125	
M8	11.7	289	2.4	271,259,125	
M9	12.5	356	0.6	271,125	
M10	13.9	342	1.2	256,257,125	
M11	11.2	288	1.7	271,125	
M12	12.5	243	1.6	125	
M13	10.8	502	2.4	326	255
M14	10.6	518	2.5	342	271,125
M15	11.3	532	2.4	356	271,125
M16	12.6	532	1.9	338	255,125
M17	11.8	449	2.6	273	255,125
M18	10.6	548	2.1	530	372,271
M19	10.4	332*	0.2	356	271,125

Supplemental Table 2. The amount of clemizole and metabolites present after 20 mM clemizole was incubated with human, rat or mouse liver microsomes for 1 hr; or after incubation with rat or human hepatocytes for 30 minutes. The number indicates the % of the total identified metabolites. None of these metabolites were detected in control incubations. ND indicates that a metabolite was not detected

	Microsomes			Hepatocytes	
	Human	Rat	Mouse	Human	Rat
Clem	40.1	3	24.1	15	ND
M1	35.5	3.5	2.5	39	ND
M2	1.8	3.5	4.8	0.1	ND
M3	4.6	6.1	5.7	0.2	ND
M4	5.4	4.8	3.4	4	ND
M5	4	6.8	2.5	0.5	ND
M6	2.3	2.7	1.8	18	ND
M7	1	5.3	0.7	4.7	ND
M8	0.3	17.9	9.8	ND	ND
M9	2.9	37.1	19.2	4	1.1
M10	1.3	ND	ND	ND	3.7
M11	0.2	9.3	25.5	ND	ND
M12	0.6	ND	ND	1.2	1.1
M13	ND	ND	ND	3	ND
M14	ND	ND	ND	10	5.4
M15	ND	ND	ND	0.3	43.6
M16	ND	ND	ND	ND	13.1
M17	ND	ND	ND	ND	10.2
M18	ND	ND	ND	ND	10.9
M19	ND	ND	ND	ND	10.9

Supplemental Table 3. The identified metabolites present after incubation of the indicated concentration of 10 uM clemizole with the indicated expressed recombinant human CYP450 for 20 min. The minor Phase 1 metabolites M5-M12 were not observed in the CYP450 phenotyping experiments.

CYP450:	<u>1a2</u>	<u>2b6</u>	<u>2c8</u>	<u>2c9</u>	<u>2c19</u>	<u>2d6</u>	<u>3a4</u>
Metabolites:	M2	M2	M2	M2	M2	M1	M1
	M4			M4		M2	M2

Supplemental Table 4. The age and sex of the 6 different human hepatocyte donors whose cells were used to produce 8 chimeric mice are shown, along with the human serum albumin level measured at the time when the pharmacokinetic experiments were performed. The percentage of the liver that is humanized, which was calculated based upon the measured albumin level as described in (Hasegawa et al., 2011), is also indicated.

<u>Human Mouse #</u>	<u>Donor Age</u>	<u>Sex</u>	<u>Hu Alb (mg/ml)</u>	<u>Human Liver (%)</u>
1	4	F	4.2	42
2	34	M	1.5	15
3	4	F	1.6	16
4	34	M	2.2	22
5	52	F	2.7	27
6	49	F	1.3	13
7	23	M	7.0	70
8	57	M	1.6	16

Supplemental Figure Legends

Supplemental Figure 1. The top graphs show the measured plasma clemizole concentration at the indicated times after a single oral 25 mg/kg dose of clemizole was administered to Balb/c or NOG mice (4 mice per group). The bottom graphs show the relative normalized abundance of clemizole and metabolites in plasma at the indicated time after dosing. As was observed in C57BL6 mice, clemizole was rapidly metabolized to 2 (M12 and M14) metabolites, while only minimal amounts of M1 or M6 were produced. The metabolite structures are shown in Figure 2.

Supplemental Figure 2. Reconstructed LC/MS chromatograms showing the relative amounts of clemizole and metabolites present after incubation of 20 uM clemizole with human, rat or mouse liver microsomes for 60 minutes. The peaks for clemizole (P), and the major human (M1) or rodent (M8, M9) metabolites are indicated.

Supplemental Figure 3. The % of clemizole remaining after 1 uM clemizole was incubated with control insect cells or with insect cells expressing the indicated recombinant CYP450 enzymes for 20 min.

Supplemental Figure 4. The relative amount of M1 produced after 20 uM clemizole was incubated with human liver microsomes in the presence of the indicated concentrations of ritonavir or omiprazole for 60 minutes.

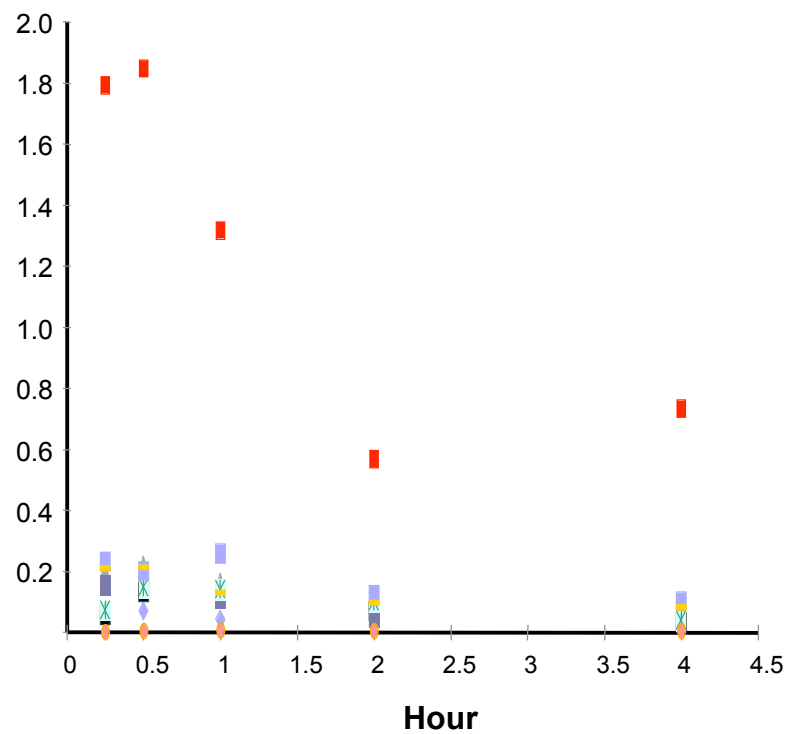
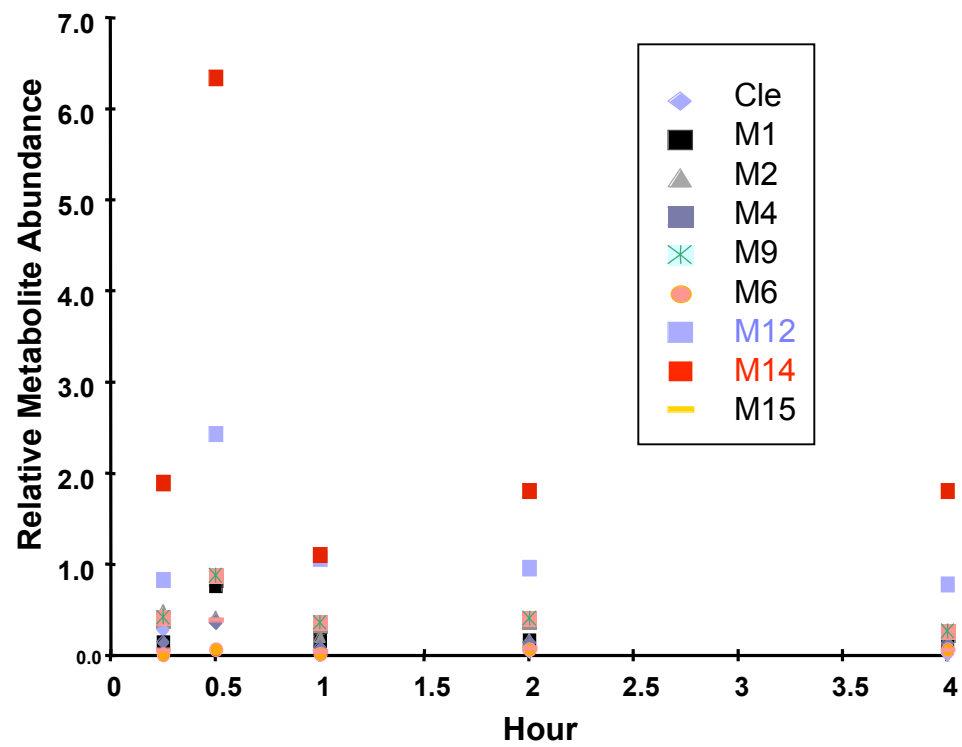
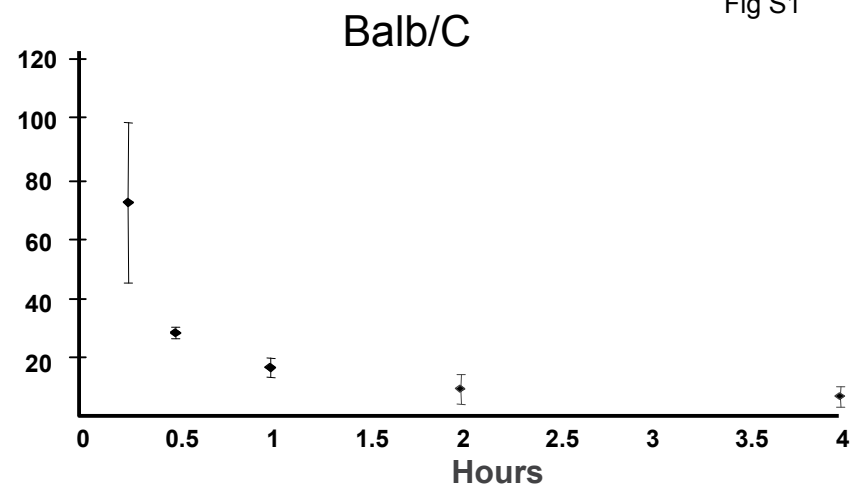
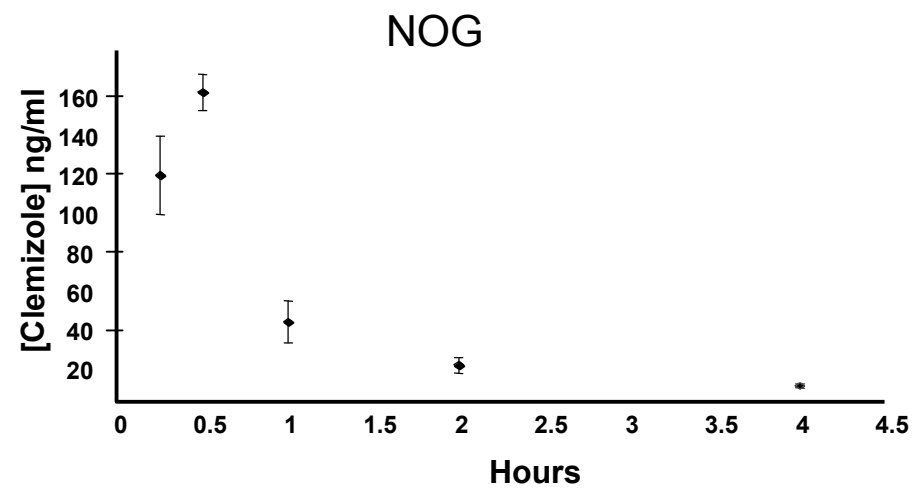


Fig S2

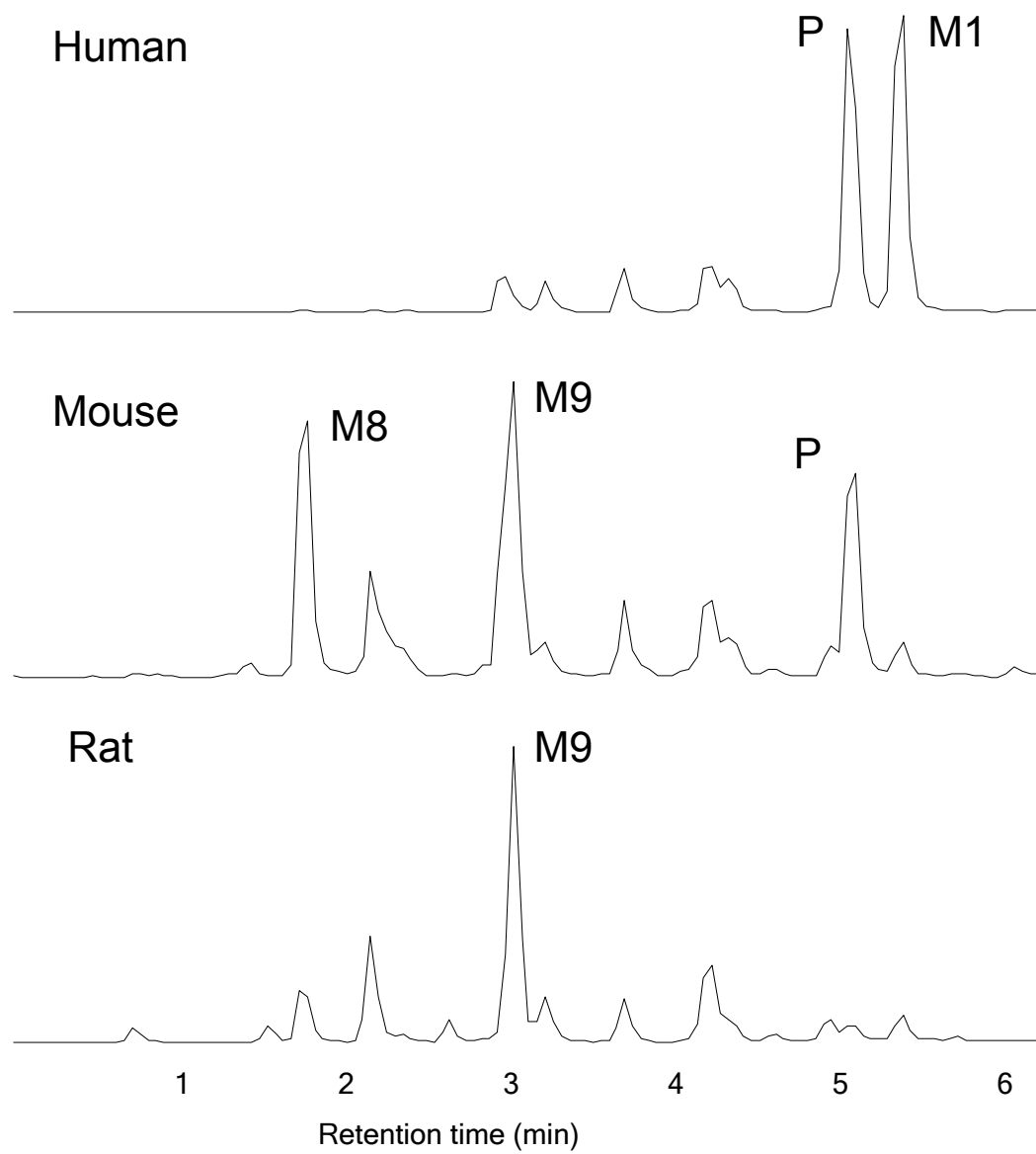


Fig S3

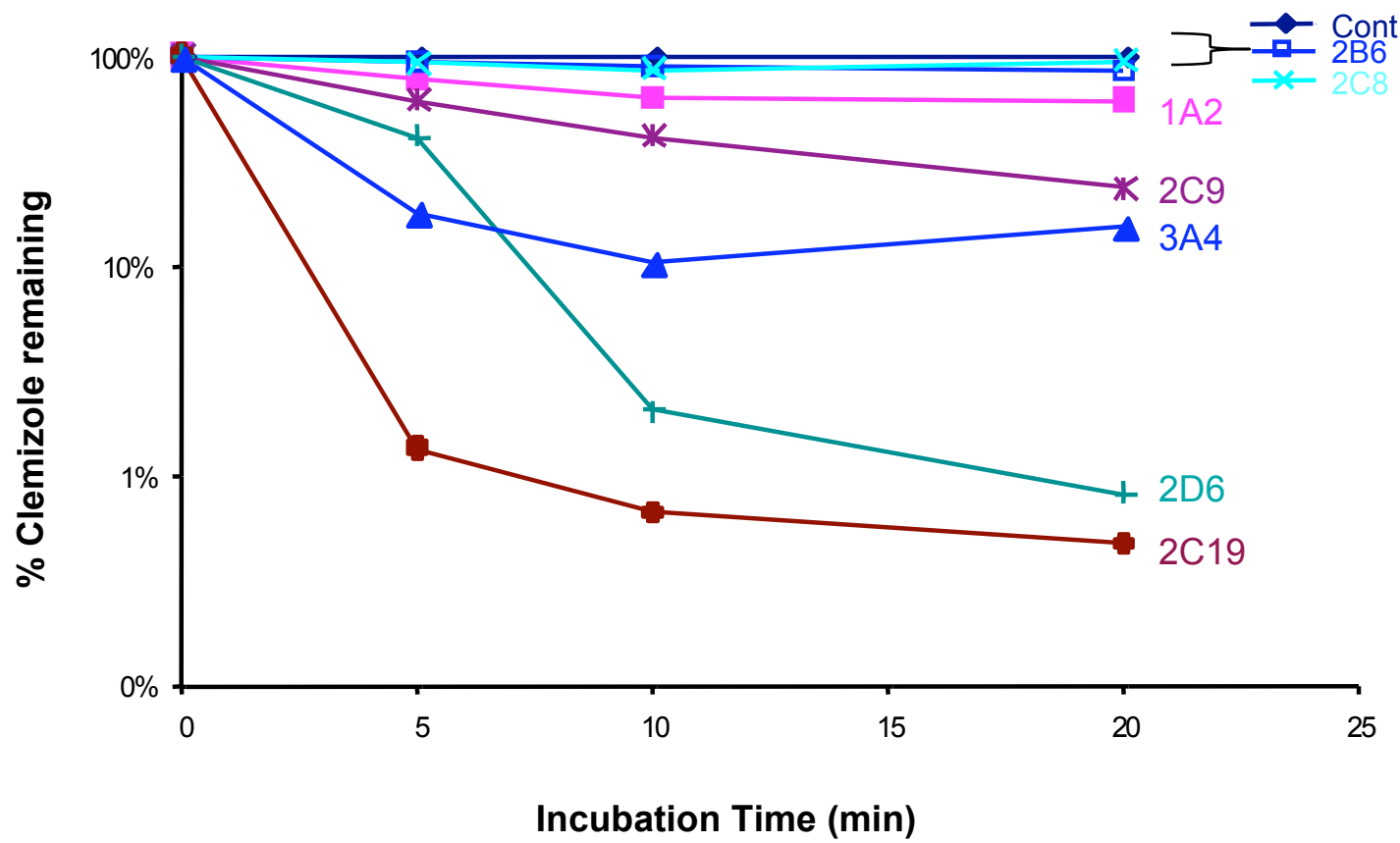


Fig S4

